PHILOSOPHICAL TRANSACTIONS OF THE ROYAL SOCIETY A MATHEMATICAL, PHYSICAL & ENGINEERING SCIENCES

Strain Coupling in the PbTiO$_{3}$ Ferroelectric Transition

K. M. Rabe and U. V. Waghmare

Phil. Trans. R. Soc. Lond. A 1996 **354**, 2897-2914
doi: 10.1098/rsta.1996.0134

Strain coupling in the $PbTiO_3$ ferroelectric transition

By K. M. Rabe and U. V. Waghmare

Department of Applied Physics, Yale University, New Haven, CT 06520-8284, USA

The construction of a first-principles effective Hamiltonian for the perovskite ferroelectric $PbTiO_3$ yields independent parameters describing separate contributions from quadratic-order lattice instabilities, anharmonic coupling, long-range dipolar interactions and strain. The origin of the large strain effects in $PbTiO_3$ is identified through analysis of chemical trends in related perovskite compounds. The generation of long-range interactions by integrating out strain is discussed for these systems, and an analogy with long-range dipolar interactions explored. The effects of strain on the finite-temperature $PbTiO_3$ ferroelectric transition are investigated by solving the effective Hamiltonian using mean field theory and the Monte Carlo simulation. Strain is found to be responsible for the stabilization of the tetragonal phase below T_c and for the first order character of the transition. The effects of strain in other perovskite transitions are expected to be similar. Finally, the importance of realistic Hamiltonians for future microscopic simulations of microstructure effects is discussed.

1. Introduction

Perovskite structure oxides show a rich variety of structural phase transitions (Lines & Glass 1977). The differing behaviour of individual compounds with changing temperature is determined by the precise balance of competing contributions from ferroelectric, antiferroelectric, and other lattice instabilities, from long-range dipolar interactions and from strain. Accurate knowledge of many independent parameters is therefore needed to obtain a description of the structural energetics useful for understanding the behaviour of particular materials and the chemical trends relating different systems.

A theoretical approach to this problem, combining quantitative realism with physical transparency, is based on the construction of effective Hamiltonians from first-principles calculations. As has been shown in recent work (Cohen & Krakauer 1992; Cohen 1992; Singh & Boyer 1992; King-Smith & Vanderbilt 1994; Zhong *et al.* 1994*a*; Rabe & Waghmare 1994; Posternak *et al.* 1994; Ghosez *et al.* 1994; Postnikov *et al.* 1994; Postnikov & Borstel 1994; Krakauer & Yu 1995; Singh 1995), the lattice instabilities and resulting structural distortions in perovskite structure oxides can be accurately calculated using first-principles density-functional methods, and the results used as the foundation of studies of the finite-temperature structural transitions (Rabe & Waghmare 1995*a*; Zhong *et al.* 1994*b*, 1995; Zhong & Vanderbilt 1995). With the lattice Wannier function method (Rabe & Waghmare 1995*b*), effective Hamiltonians can be systematically constructed even for problematic systems

Phil. Trans. R. Soc. Lond. A (1996) **354**, 2897–2914
Printed in Great Britain

involving several coupled modes at the zone boundary or interior of the zone. The resulting models are expressed in terms of easily identifiable degrees of freedom corresponding to local polar distortions and elastic deformations, and parameters which determine the energies of various types of distortions and the couplings between them. These parameters are derived from first-principles calculations for individual materials and thus provide an accurate picture of the competition between different types of instabilities and induced distortions. In particular, this approach can be used to investigate strain effects, which are very important in determining both equilibrium thermodynamic behaviour and transformation-induced microstructure in the vicinity of the structural transition (Salje 1990).

In this paper, we investigate the physics of strain and strain-induced effects at the ferroelectric transition in $PbTiO_3$ from first principles. Strain coupling operates to some degree in all perovskite structural transitions, but the strain effects in $PbTiO_3$ are observed to be especially large. It is well established (Cohen & Krakauer 1992; Cohen 1992) that strain coupling is responsible for stabilizing the tetragonal ground state structure, with $c/a = 1.06$. Here, we focus on the effects at finite temperatures, using an effective Hamiltonian which has been constructed through the lattice Wannier function method, with special attention to the treatment of strain (Rabe & Waghmare 1996; U. V. Waghmare & K. M. Rabe, unpublished work). The finite-temperature ferroelectric transition in $PbTiO_3$ is studied by applying Monte Carlo simulation and mean field theory to this effective Hamiltonian, and strain-induced effects in the transition behaviour identified by comparing the behaviour of the full system with that of the same system with strain coupling set to zero. We find that the strain coupling has a significant effect on the transition temperature and plays an important role in determining the first-order character of the phase transition, as well as stabilizing the low-temperature tetragonal phase in the full temperature range from $T = 0$ to T_c. We expect that strain coupling plays a similar role in other perovskite transitions, particularly in stabilizing intermediate temperature tetragonal phases such as those in $BaTiO_3$ (Zhong *et al.* 1994*b*, 1995) and $KNbO_3$.

The rest of this paper is organized as follows. In § 2, we present a detailed discussion of the treatment of strain degrees of freedom in the construction of effective Hamiltonians for ferroelectric $PbTiO_3$, with some comparison to aspects of the effective Hamiltonian construction for $BaTiO_3$, $KNbO_3$ and $PbZrO_3$. The origin of the large strain effects in $PbTiO_3$ is analysed in § 3. Some general considerations governing the numerical simulations of the effective Hamiltonian are discussed in § 4, with particular attention to the long-range interactions generated by strain coupling. In § 5, we present classical Monte Carlo results for $PbTiO_3$, as well as a mean field theory analysis which explicitly includes strain coupling. The prospects for future studies of the effects of spatial fluctuations and inhomogeneities using these realistic effective Hamiltonians are discussed in § 6. Section 7 concludes the paper.

2. Effective Hamiltonian

For the construction of the effective Hamiltonians for the ferroelectric transition in $PbTiO_3$, we use the lattice Wannier function method (Rabe & Waghmare 1995*b*). Complete descriptions of the effective Hamiltonian constructions for $PbTiO_3$ and the more complicated antiferroelectric $PbZrO_3$ are contained in Rabe & Waghmare (1996) and Waghmare & Rabe (1996). Here, we focus on the treatment of the strain

PHILOSOPHICAL TRANSACTIONS OF THE ROYAL SOCIETY A MATHEMATICAL, PHYSICAL & ENGINEERING SCIENCES

degrees of freedom and the coupling of strain to other local distortions in $PbTiO_3$, with comparisons to related features of $BaTiO_3$, $KNbO_3$ and $PbZrO_3$.

In the lattice Wannier function method, the effective Hamiltonian is obtained as the result of projection of the full lattice Hamiltonian (in the Born–Oppenheimer approximation) into a subspace of the full ionic displacement space. Starting from a high-symmetry reference configuration (in this case, the cubic perovskite structure), an orthonormal basis of symmetrized localized atomic displacement patterns, called 'lattice Wannier functions', is constructed to span the effective Hamiltonian subspace. This basis defines a set of coordinates such that a non-zero value of one of the coordinates corresponds directly to a particular localized pattern of atomic displacements with definite symmetry. The effective Hamiltonian can be written as a function of these coordinates. As a result of the symmetrized and localized nature of the basis, the Taylor expansion of the effective Hamiltonian around the high-symmetry reference configuration (with all coordinate values equal to zero) has a simple form with relatively few parameters, which can be determined from first-principles calculations using the correspondence to patterns of atomic displacements.

The symmetry properties of a lattice Wannier function are specified by a Wyckoff symbol for the space group of the high-symmetry reference structure and an irreducible representation of the corresponding site symmetry group. For a given symmetry type of lattice Wannier function, a parametrization of the localized atomic displacement pattern is obtained by choosing one of the Wyckoff positions specified by the Wyckoff symbol, finding the symmetric coordination shells surrounding that site and identifying the independent displacement patterns of each shell that transform according to the given irreducible representation of the site symmetry group. For a particular system, the lattice Wannier function symmetries are chosen and atomic displacement pattern parameters adjusted so that the subspace spanned contains the desired set of phonons, with eigenvectors obtained from first-principles calculations of the dynamical matrix. This set includes both the 'relevant' phonons, which freeze into a high-symmetry reference structure (in this case, the cubic perovskite structure) to produce the low-temperature structure, and the lowest energy phonons of appropriate symmetry at other points in the Brillouin zone.

For the Γ_{15} ferroelectric transition found in $PbTiO_3$, the lattice Wannier function symmetry is that of a vector centred on the A site (Rabe & Waghmare 1996; U. V. Waghmare & K. M. Rabe, unpublished work). For the closely related Γ_{15} ferroelectric transitions in $BaTiO_3$ (Zhong *et al.* 1994*b*, 1995) and $KNbO_3$ (H. Krakauer and others, unpublished work), the lattice Wannier function has the symmetry of a vector centred on the B site. The choice of A versus B-centred vectors, both of which span subspaces containing Γ_{15}, is determined by the symmetry labels of the lowest zone-boundary modes in each material. For antiferroelectric $PbZrO_3$, there are four relevant phonons: an R_{25} oxygen-octahedron rotation, a Γ_{15} polar mode, a $(\frac{1}{2}\frac{1}{2}0)(\pi/a)\Sigma_3$ mode, and a $(110)(\pi/a)M_5'$ mode (Cochran & Zia 1968). The symmetry labels of all these modes can be reproduced by a basis of lattice Wannier functions with the symmetry of two-dimensional vectors centred on the oxygen sites. However, to reproduce the first-principles eigenvectors of all the relevant modes with well-localized lattice Wannier functions, it proves necessary to extend the basis to include lattice Wannier functions with the symmetry of vectors centred on the A site. As we will discuss further later, there then remain degrees of freedom in the oxygen-centred subspace which can be used to represent inhomogeneous strain.

With this choice of basis, the effective Hamiltonian for $PbTiO_3$ describes a system

PHILOSOPHICAL TRANSACTIONS OF THE ROYAL SOCIETY A MATHEMATICAL, PHYSICAL & ENGINEERING SCIENCES

of three-dimensional vectors $\{\boldsymbol{\xi}_i\}$ at the sites of a simple cubic lattice. $\mathcal{H}_{\text{eff}}$ is expanded in symmetry-invariant combinations with respect to O_h^1, the space group of the cubic perovskite structure. In the present work, intercell interactions are included up to quadratic order only. For first, second and third neighbours, the most general quadratic interactions allowed by symmetry are included:

$$\frac{1}{N}\sum_i \sum_{\hat{d}=nn1} [a_{\mathrm{L}}(\boldsymbol{\xi}_i\cdot\hat{d})(\boldsymbol{\xi}_i(\hat{d})\cdot\hat{d}) + a_T(\boldsymbol{\xi}_i\cdot\boldsymbol{\xi}_i(\hat{d}) - (\boldsymbol{\xi}_i\cdot\hat{d})(\boldsymbol{\xi}_i(\hat{d})\cdot\hat{d}))], \tag{2.1}$$

$$+\frac{1}{N}\sum_i \sum_{\hat{d}=nn2} [b_{\mathrm{L}}(\boldsymbol{\xi}_i\cdot\hat{d})(\boldsymbol{\xi}_i(\hat{d})\cdot\hat{d}) + b_{T1}(\boldsymbol{\xi}_i\cdot\hat{d}_1)(\boldsymbol{\xi}_i(\hat{d})\cdot\hat{d}_1) + b_{T2}(\boldsymbol{\xi}_i\cdot\hat{d}_2)(\boldsymbol{\xi}_i(\hat{d})\cdot\hat{d}_2)], \tag{2.2}$$

$$+\frac{1}{N}\sum_i \sum_{\hat{d}=nn3} [c_{\mathrm{L}}(\boldsymbol{\xi}_i\cdot\hat{d})(\boldsymbol{\xi}_i(\hat{d})\cdot\hat{d}) + c_T(\boldsymbol{\xi}_i\cdot\boldsymbol{\xi}_i(\hat{d}) - (\boldsymbol{\xi}_i\cdot\hat{d})(\boldsymbol{\xi}_i(\hat{d})\cdot\hat{d}))], \tag{2.3}$$

while beyond third neighbour we use a dipole–dipole form parametrized by the mode effective charge $\overline{Z}^*$ and the electronic dielectric constant ϵ_∞:

$$\frac{1}{N}\sum_i \sum_{\boldsymbol{d}} \frac{(\overline{Z}^*)^2}{\epsilon_\infty} \frac{(\boldsymbol{\xi}_i\cdot\boldsymbol{\xi}_i(\hat{d}) - 3(\boldsymbol{\xi}_i\cdot\hat{d})(\boldsymbol{\xi}_i(\hat{d})\cdot\hat{d}))}{|\boldsymbol{d}|^3}. \tag{2.4}$$

Terms in the onsite potential, depending only on values of $\boldsymbol{\xi}_i$ at a single i, include isotropic terms up to eighth order in $|\boldsymbol{\xi}_i|$ and full cubic anisotropy at fourth order:

$$\frac{1}{N}\sum_i (A|\boldsymbol{\xi}_i|^2 + B|\boldsymbol{\xi}_i|^4 + C(\xi_{ix}^4 + \xi_{iy}^4 + \xi_{iz}^4) + D|\boldsymbol{\xi}_i|^6 + E|\boldsymbol{\xi}_i|^8). \tag{2.5}$$

Uniform distortions of the underlying lattice are easily included by introducing the six-component homogeneous strain tensor $e_{\alpha\beta}$ ($\alpha,\beta = x,y,z$). The energy associated with homogeneous strain and its coupling to the local distortion $\boldsymbol{\xi}_i$ is included in our effective Hamiltonian for $PbTiO_3$ to lowest non-trivial order:

$$\tfrac{1}{2}C_{11}\sum_\alpha e_{\alpha\alpha}^2 + \tfrac{1}{2}C_{12}\sum_{\alpha\neq\beta} e_{\alpha\alpha}e_{\beta\beta} + \tfrac{1}{4}C_{44}\sum_{\alpha\neq\beta} e_{\alpha\beta}^2 + f\sum_\alpha e_{\alpha\alpha}, \tag{2.6}$$

$$+\frac{g_0}{N}\left(\sum_\alpha e_{\alpha\alpha}\right)\sum_i |\boldsymbol{\xi}_i|^2 + \frac{g_1}{N}\sum_\alpha \left(e_{\alpha\alpha}\sum_i \xi_{i\alpha}^2\right) + \frac{g_2}{N}\sum_{\alpha<\beta} e_{\alpha\beta}\sum_i \xi_{i\alpha}\xi_{i\beta}. \tag{2.7}$$

For our calculations in $PbTiO_3$, we take $e_{\alpha\beta} = 0$ at $a_0 = 3.968\,83$ Å, the lattice constant measured for the cubic phase just above T_c.

When coupling to homogeneous strain is important, then the fluctuations and spatial inhomogeneity associated with inhomogeneous strain also can be expected to be important. For inhomogeneous strain, the 'relevant phonons' are the zero-frequency acoustic modes at the zone centre. In the lattice Wannier function method, the inhomogeneous strain is represented by three degrees of freedom per unit cell, corresponding to a displacement field. Each degree of freedom represents the collective motion of a group of atoms, and if the values are chosen to be uniform, the corresponding ionic configuration is a uniform translation of the whole crystal. Away from the zone centre, the acoustic modes are reproduced by a suitable choice of atomic displacement pattern parameters. In this representation, we expand the pure strain Hamiltonian in symmetry-invariant combinations. At quadratic order, the coefficients

in this expansion are force constants, which we truncate at some chosen range, and higher-order couplings (if included) are also truncated at short range. Note that the displacement pattern for the strain lattice Wannier functions has no net dipole moment, so that it is not necessary to include long-range dipolar interactions. To ensure the preservation of global translational and rotational invariance within a force constant model, we use the construction of Keating (1966). Since the lattice Wannier functions are fit to the calculated phonon dispersions, the lowest-order interactions between local distortion variables and strain are anharmonic. Typically, we include the shortest-range lowest-order interactions only, imposing the constraint that a uniform translation cannot lead to a change in energy at any order.

The construction of the pure strain Hamiltonian for $PbTiO_3$ is relatively simple. To include inhomogeneous strain, the basis is expanded to include lattice Wannier functions with the symmetry of vectors centred on the B site. As described previously, the atomic displacement patterns must reproduce the Γ_{15} uniform translation modes. If the expansion of the effective Hamiltonian in the Keating construction is truncated at three independent parameters and quadratic order, corresponding to the three elastic constants, the following Hamiltonian terms are obtained:

$$\frac{1}{N}\sum_i \tilde{A}|\boldsymbol{u}_i|^2, \tag{2.8}$$

$$+\frac{1}{N}\sum_i\sum_{\hat{d}=nn1}[\tilde{a}_{\mathrm{L}}(\boldsymbol{u}_i\cdot\hat{d})(\boldsymbol{u}_i(\hat{d})\cdot\hat{d})+\tilde{a}_T(\boldsymbol{u}_i\cdot\boldsymbol{u}_i(\hat{d})-(\boldsymbol{u}_i\cdot\hat{d})(\boldsymbol{u}_i(\hat{d})\cdot\hat{d}))], \tag{2.9}$$

$$+\frac{1}{N}\sum_i\sum_{\hat{d}=nn2}[\tilde{b}_{\mathrm{L}}(\boldsymbol{u}_i\cdot\hat{d})(\boldsymbol{u}_i(\hat{d})\cdot\hat{d})+\tilde{b}_{T1}(\boldsymbol{u}_i\cdot\hat{d}_1)(\boldsymbol{u}_i(\hat{d})\cdot\hat{d}_1)+\tilde{b}_{T2}(\boldsymbol{u}_i\cdot\hat{d}_2)(\boldsymbol{u}_i(\hat{d})\cdot\hat{d}_2)]. \tag{2.10}$$

With the expression of these parameters in terms of the elastic constants

$$\tilde{A}=C_{11}+2C_{44},$$
$$\tilde{a}_{\mathrm{L}}=-\tfrac{1}{2}C_{11},$$
$$\tilde{a}_T=-\tfrac{1}{2}C_{44},$$
$$\tilde{b}_{\mathrm{L}}=-\tilde{b}_{T1}=-\tfrac{1}{8}C_{12}+\tfrac{1}{24}C_{44},$$
$$\tilde{b}_{T2}=0,$$

they can easily be obtained from first-principles calculations. Because there are no unstable modes in this subspace, there is no need to include higher-order interactions. However, additional quadratic parameters could be included to improve the description of the acoustic modes away from the zone centre.

The construction of the terms in the $PbTiO_3$ effective Hamiltonian coupling strain and local distortions is also rather simple. With Wannier basis vectors that exactly reproduce the phonon eigenvectors, there is no quadratic coupling between the two subspaces A and B. The simplest anharmonic coupling that satisfies the constraint of global translational invariance and does not vanish in the limit $\boldsymbol{k}\rightarrow 0$ are the nearest-neighbour couplings linear in $\boldsymbol{u}$ and quadratic in $\boldsymbol{\xi}$, with both ξ variables

taken on the same site:

$$\frac{\tilde{h}_0}{N}\sum_i\left\{\xi_{ix}^2\sum_{\boldsymbol{d}=\pm\hat{y}\pm\hat{z}}(u_x(\boldsymbol{R}_i+\tfrac{1}{2}a_0\hat{x}+\tfrac{1}{2}a_0\boldsymbol{d})-u_x(\boldsymbol{R}_i-\tfrac{1}{2}a_0\hat{x}+\tfrac{1}{2}a_0\boldsymbol{d}))+\text{c.p.}\right\}$$
$$+\frac{\tilde{h}_1}{N}\sum_i\left\{\xi_{ix}^2\left(\sum_{\boldsymbol{d}=\pm\hat{x}\pm\hat{z}}(u_y(\boldsymbol{R}_i+\tfrac{1}{2}a_0\hat{y}+\tfrac{1}{2}a_0\boldsymbol{d})-u_y(\boldsymbol{R}_i-\tfrac{1}{2}a_0\hat{y}+\tfrac{1}{2}a_0\boldsymbol{d}))\right.\right.$$
$$\left.\left.+\sum_{\boldsymbol{d}=\pm\hat{x}\pm\hat{y}}(u_z(\boldsymbol{R}_i+\tfrac{1}{2}a_0\hat{z}+\tfrac{1}{2}a_0\boldsymbol{d})-u_z(\boldsymbol{R}_i-\tfrac{1}{2}a_0\hat{z}+\tfrac{1}{2}a_0\boldsymbol{d}))\right)+\text{c.p.}\right\}$$
$$+\frac{\tilde{h}_2}{N}\sum_i\left\{\xi_{ix}\xi_{iy}\left(\sum_{\boldsymbol{d}=\pm\hat{x}\pm\hat{z}}(u_x(\boldsymbol{R}_i+\tfrac{1}{2}a_0\hat{y}+\tfrac{1}{2}a_0\boldsymbol{d})-u_x(\boldsymbol{R}_i-\tfrac{1}{2}a_0\hat{y}+\tfrac{1}{2}a_0\boldsymbol{d}))\right.\right.$$
$$\left.\left.+\sum_{\boldsymbol{d}=\pm\hat{y}\pm\hat{z}}(u_y(\boldsymbol{R}_i+\tfrac{1}{2}a_0\hat{x}+\tfrac{1}{2}a_0\boldsymbol{d})-u_y(\boldsymbol{R}_i-\tfrac{1}{2}a_0\hat{x}+\tfrac{1}{2}a_0\boldsymbol{d}))\right)+\text{c.p.}\right\}.$$

ξ^2 couples only to differences of u, which can be recognized as finite difference approximations to the gradient, and thus as the local strain tensor (also used in Zhong *et al.* (1994*b*, 1995)). The three independent coupling parameters can be obtained from first-principles calculations of the change in the quadratic part of the energy of a uniform local distortion with changes in homogeneous strain (Rabe & Waghmare 1996; U. V. Waghmare & K. M. Rabe, unpublished work).

For $PbZrO_3$, the larger number of lattice Wannier functions per unit cell leads to considerably more complicated expressions for the effective Hamiltonian, which are given in detail in Waghmare & Rabe (1996). The situation regarding strain is somewhat different than in $PbTiO_3$, since the inhomogeneous strain degrees of freedom are in the $6N$-dimensional subspace of two-dimensional vectors centred on the oxygen sites. In this case, we compute the quadratic parameters by fitting to first-principles phonon eigenvectors and building into the fit the relations between the parameters obtained by directly imposing the constraint of overall translational invariance. Because of the presence of unstable modes in the oxygen-centred subspace, it is also necessary to include fourth-order interactions. For these parameters we also obtain relations from the requirement of translational invariance, leading to a set of short-range onsite and intersite interactions which are fit to anharmonic energies obtained from first-principles total-energy calculations for uniform and selected zone-boundary distortions. As in $PbTiO_3$, the Pb-centred vector lattice Wannier functions also have anharmonic couplings to strain. The leading-order parameters are extracted from first-principles calculations of the coupling of uniform distortions to homogeneous strain by a procedure closely related to that in $PbTiO_3$.

There are a number of interesting points of comparison between our method for constructing effective Hamiltonians and the approach to microscopic modelling of structural phase transitions in minerals developed in Marais *et al.* (1991), Salje (1992) and Marais *et al.* (1994). As in the present discussion, the strain is treated at the microscopic level, modelled by a system of atoms connected by springs, building in global translational and rotational invariance. The main distinction is in the character of the local distortion variables. In the work on minerals, the local distortions are Ising variables, for example representing two possible orientation states of a local cluster. In the present discussion of perovskites, all local distortions are variable length vectors. This leads to significantly different symmetry restrictions on the allowed terms that

couple local distortions and strain. In the minerals mainly considered, the leading order coupling is bilinear, generating long-range quadratic interactions between local distortions when the strain is integrated out (Bratkovsky *et al.* 1994; Tsatkis *et al.* 1994). In the perovskites, the leading order coupling is linear in strain and quadratic in the local distortion, so that the induced long-range interactions are quartic, as will be described in more detail in § 4.

It should be possible, however, to improve the connections between these two approaches. The lattice Wannier function method can, in principle, also be applied to systems with chemical disorder and to systems with discrete local distortions, both of which will require the inclusion of Ising-like variables. In such systems, the resulting effective Hamiltonians should be closely related to those previously obtained for minerals, and instructive comparisons should be possible.

3. Ground state structure determination

In this section, we examine the energetics of strain coupling in $PbTiO_3$ and other perovskites within the effective Hamiltonian framework. The goal is to understand, in particular, whether the observation of large strain in the low temperature phase of $PbTiO_3$ is due to any unusual features of the structural energetics, such as anomalous elastic constants or strain couplings, that can be identified by examining chemical trends in this class of materials. For this analysis, we use the first-principles effective-Hamiltonian parameters which describe uniform distortions in eight perovskite compounds ($BaTiO_3$, $SrTiO_3$, $CaTiO_3$, $KNbO_3$, $NaNbO_3$, $PbTiO_3$, $PbZrO_3$ and $BaZrO_3$) from table I of King-Smith & Vanderbilt (1994).

A simple quantification of the importance of strain coupling, suggested by Salje (1990), is the fraction of total distortion energy contributed by the strain relaxation. For each of the eight perovskite compounds, we calculated the fraction of the total energy difference between the cubic and the optimal tetragonal phase contributed by the strain relaxation. In $PbTiO_3$, we find this fraction to be 0.5, comparable to the highest excess Gibbs free energy fractions observed in known ferroelastic minerals. However, this is not a distinguishing feature of $PbTiO_3$, since six of the seven other perovskites included in the table have similar values, in the range 0.38–0.51. Only $PbZrO_3$ is different, with a significantly lower value of 0.18.

The role of strain coupling which has been most discussed in the literature is that of determining whether the tetragonal or rhombohedral structure is the ground-state structure. In the work of Cohen & Krakauer (Cohen & Krakauer 1992; Cohen 1992), strain coupling was seen to enhance the stability of the tetragonal phase both in $PbTiO_3$ and $BaTiO_3$. In both cases, the ground-state structure in the absence of strain coupling is rhombohedral. The magnitudes of the stability enhancement result in a ground-state tetragonal structure in $PbTiO_3$, while in $BaTiO_3$ the rhomobohedral structure remains most stable. This comparison can be conveniently made by integrating out the strain energy for uniform distortions to obtain effective fourth-order couplings, as is described in detail in § II of King-Smith & Vanderbilt (1994), resulting in the following expression for the energy:

$$E(\boldsymbol{\xi}) = \kappa|\boldsymbol{\xi}|^2 + \alpha'|\boldsymbol{\xi}|^4 + \gamma'(\xi_x^2\xi_y^2 + \xi_x^2\xi_z^2 + \xi_y^2\xi_z^2).$$

The tetragonal structure is favoured if the fourth-order anisotropy γ' is positive, and the rhombohedral favoured if γ' is negative. The signs for γ' obtained for $PbTiO_3$

and $BaTiO_3$ in King-Smith & Vanderbilt (1994) are consistent with the results of Cohen & Krakauer (1992) and Cohen (1992) described previously.

The expression for γ' in terms of elastic constants and couplings between local distortions and strains is

$$\gamma' = \gamma + \frac{1}{2}\left(\frac{\nu_t^2}{\mu_t} - \frac{\nu_r^2}{\mu_r}\right),$$

where μ_t and μ_r are tetragonal and rhombohedral shear moduli, and ν_t and ν_r are the corresponding strain couplings. Examination of this expression shows that the differences between $PbTiO_3$ and $BaTiO_3$ are in fact rather subtle. In both cases, γ' is the sum of a negative bare contribution γ and a positive contribution from coupling to tetragonal strain $\frac{1}{2}(\nu_t^2/\mu_t)$ which are comparable in magnitude (the contribution from coupling to rhombohedral strain $-\frac{1}{2}(\nu_r^2/\mu_r)$ is negligible). In $PbTiO_3$, the tetragonal strain coupling contribution is slightly larger in magnitude than γ, resulting in a tetragonal ground state, while in $BaTiO_3$, it is slightly smaller, resulting in a rhombohedral ground state. As a result of this near cancellation, which occurs for all eight perovskites studied, we have not been able to identify any systematic correlations in the sign or relative magnitude of γ' with quantities such as the relevant elastic constant μ_t, the ratio ν_t^2/γ, or the frustration δ. In particular, the tetragonal shear modulus μ_t and the ratio ν_t^2/γ are not dramatically different between $PbTiO_3$ and $BaTiO_3$ (μ_t is slightly smaller for $PbTiO_3$ and ν_t^2/γ slightly larger).

The upshot of this discussion is that the elastic constants and strain couplings in $PbTiO_3$ are not anomalous when compared to those of $BaTiO_3$ and other perovskites. The fact remains, however, that the structural transitions in $PbTiO_3$ and $BaTiO_3$ seem quite different. In particular, a comparison of the latent heats at the cubic–tetragonal transition shows a pronounced distinction between the two compounds, which can be roughly correlated with the energy difference between the cubic and optimal tetragonal structures $\kappa^2/(4\alpha')$. This latter trend does not directly arise from differences in strain parameters, but rather from the very different values of bare α, which is much smaller in $PbTiO_3$ than in $BaTiO_3$. The much smaller α in $PbTiO_3$ is also responsible for the much larger amplitude for the local distortion in the optimal tetragonal structure, as seen in Cohen & Krakauer (1992) and Cohen (1992). The large tetragonal distortion in the ground state comes from the coupling of this strain to the large local distortion, according to

$$e_{zz}^{(0)} - e_{xx}^{(0)} = -\frac{g_1}{C_{11} - C_{12}}(\xi_z^{(0)})^2.$$

The difference in the values of α in the two compounds can be accounted for by examination of the unstable mode eigenvectors. To within 5%, the fourth-order energy for the local distortion in the unstrained tetragonal structure for the two compounds has the same value for a given distance between Ti and the nearest apical oxygen, i.e.

$$\frac{\alpha(\mathrm{Pb})}{\alpha(\mathrm{Ba})}\left(\frac{1.28a_0(\mathrm{Ba})}{0.78a_0(\mathrm{Pb})}\right)^4 = 1.05.$$

Because of the larger involvement of Pb in the unstable mode in $PbTiO_3$, this given distance corresponds to a significantly larger local distortion amplitude. The significant role of Pb in the lattice instability has been previously noted (Cohen & Krakauer 1992; Cohen 1992; Rabe & Waghmare 1996; U. V. Waghmare & K. M. Rabe, unpublished work), and can be attributed to the unique chemistry of divalent Pb in oxides.

PHILOSOPHICAL TRANSACTIONS OF THE ROYAL SOCIETY A MATHEMATICAL, PHYSICAL & ENGINEERING SCIENCES

In conclusion, it is not the strain parameters that are anomalous in $PbTiO_3$, but the anharmonic energy for the local distortion. The resulting large effects, however, make $PbTiO_3$ ideal for studying strain-related effects at the structural transitions which are present to some degree in all the perovskite transitions. As we shall discuss in more detail later, the strain coupling turns out to play a crucial role in determining the behaviour at the finite-temperature transition in $PbTiO_3$, and likely in many other systems as well.

4. Finite temperature simulations: general considerations

The form of the effective Hamiltonian, while greatly simplified relative to the original lattice Hamiltonian, is still sufficiently complicated to discourage the application of analytical statistical mechanics methods such as renormalization group analysis or high-temperature expansions. However, it is quite suitable for Monte Carlo simulation, since changes in energy with configuration are readily calculated numerically (Allen & Tildesley 1987). In a classical Monte Carlo simulation, thermodynamic properties and probability distributions characterizing local structure can be calculated with the assistance of finite-size scaling, permitting identification and investigation of finite-temperature structural transitions of the system. Ideally, the size of the simulation cell should be large enough to allow for the spatial inhomogeneity and domain structure considered to play an important role in the experimentally observed behaviour of these materials (Zhang *et al.* 1994). However, it has not yet been possible to perform such simulations for the $PbTiO_3$ effective Hamiltonian. The main obstacle to performing simulations for very large finite-size systems is the evaluation of the energy from the long-range dipole interaction, which will be discussed later in this section.

The treatment of the strain variables in classical Monte Carlo simulations deserves specific comment. Because the strain variables appear only to quadratic order in the $PbTiO_3$ effective Hamiltonian, it is possible to integrate over them analytically to obtain a reduced Hamiltonian expressed only in terms of the local distortion variables. Performing these integrals analytically rather than numerically seems to offer advantages both for the computation and for the physical interpretation of the behaviour of the system (Marais *et al.* 1991). However, the analytical integration generates long-range anisotopic quartic interaction terms in the local distortion variables. This can easily be seen for homogeneous strain by diagonalizing the quadratic term in $e_{\alpha\beta}$ in equation (2.6) through transformation to the symmetrized variables $v_1 = (1\sqrt{3})(e_{xx}+e_{yy}+e_{zz})$, $v_2 = (1\sqrt{2})(e_{xx}-e_{yy})$ and $v_3 = (1\sqrt{6})(-e_{xx}-e_{yy}+2e_{zz})$. The terms in the Hamiltonian that depend on homogeneous strain (equations (2.6) and (2.7)) then take the form

$$\begin{aligned}
&\tfrac{1}{2}(C_{11}+2C_{12})v_1^2 + \tfrac{1}{2}(C_{11}-C_{12})(v_2^2+v_3^2) + 2C_{44}(e_{xy}^2+e_{xz}^2+e_{yz}^2)\\
&\quad+\frac{\sqrt{3}\tilde{b}}{N}\left(\sum_i \boldsymbol{\xi}_i^2\right)v_1 + \frac{\tilde{a}}{N\sqrt{2}}\left(\sum_i \xi_{ix}^2 - \sum_i \xi_{iy}^2\right)v_2\\
&\quad+\frac{\tilde{a}}{N\sqrt{6}}\left(-\sum_i \xi_{ix}^2 - \sum_i \xi_{iy}^2 + 2\sum_i \xi_{iz}^2\right)v_3,
\end{aligned}$$

where $\tilde{a} = g_1$ and $\tilde{b} = g_0 + \frac{1}{3}g_1$. The three one-dimensional Gaussian integrals in the partition function are then easily evaluated, with the resulting contribution to the

reduced effective Hamiltonian (still temperature independent):

$$\left[\frac{-3\tilde{b}^2}{2(C_{11}+2C_{12})}+\frac{\tilde{a}^2}{6(C_{11}-C_{12})}\right]\left(\frac{1}{N}\sum_i|\boldsymbol{\xi}_i|^2\right)^2$$
$$-\frac{\tilde{a}^2}{2(C_{11}-C_{12})}\left(\left(\frac{1}{N}\sum_i\xi_{ix}^2\right)^2+\left(\frac{1}{N}\sum_i\xi_{iy}^2\right)^2+\left(\frac{1}{N}\sum_i\xi_{iz}^2\right)^2\right)$$
$$-\frac{g_2^2}{2C_{44}}\left[\left(\frac{1}{N}\sum_i\xi_{ix}\xi_{iy}\right)^2+\left(\frac{1}{N}\sum_i\xi_{ix}\xi_{iz}\right)^2+\left(\frac{1}{N}\sum_i\xi_{iy}\xi_{iz}\right)^2\right].$$

While in the case of homogeneous strain, the anisotropic quartic interactions thus generated are infinite range and independent of separation, the analogous integration of inhomogeneous strain will produce long range interactions which are separation dependent. Note that this same symmetry-based change of variables also facilitates the integration of the homogeneous strain coupled to uniform local distortions, as described in § 3.

These long-range anisotopic quartic interaction terms in the reduced Hamiltonian significantly complicate the calculation of change in energy with change in configuration. There is therefore a trade-off between reduction in the number of degrees of freedom and range of the interactions. For this reason, in our Monte Carlo investigation of the ferroelectric transition in $PbTiO_3$, we have decided to retain both the local and homogeneous strain variables explicitly. Only for the homogeneous strain are the induced interactions simple to calculate, and we have found that the results from both approaches are the same.

The example of strain coupling in generating anisotropic long-range interactions suggests a possible method for attacking the problem of computing the energy contribution of dipolar interaction terms. We have found that it is possible to construct partition-function-like integrals for systems of local distortions and auxiliary variables such that when the auxiliary variables are integrated out, the long-range dipolar interaction is generated (B. A. Elliott & K. M. Rabe, unpublished work). In the argument of the exponential, the auxiliary field variables appear to quadratic order only (permitting analytical integration) and interactions between all variables are short range, eliminating the long-range interactions so problematic in the numerical simulations. For example, for vector variables $\boldsymbol{\xi}_j$ on the sites of a simple cubic lattice, we introduce a scalar auxiliary field ϕ_j at each lattice site, and write

$$Z=\int\{\mathrm{d}\phi_j\}\int\{\mathrm{d}\boldsymbol{\xi}_j\}\exp(-\beta[\mathcal{H}_0(\{\boldsymbol{\xi}_j\})+\mathcal{H}_1(\{\phi_j\})+\mathrm{i}\mathcal{H}_{\mathrm{int}}(\{\boldsymbol{\xi}_j\},\{\phi_j\})]),$$

where all terms include only short-range interactions allowed by cubic symmetry, $\mathcal{H}_1$ is purely quadratic, and $\mathcal{H}_{\mathrm{int}}$ is the sum of the symmetry-allowed bilinear coupling terms between ϕ_j and the independent short-range finite-difference approximations to $\nabla\cdot\boldsymbol{\xi}$ evaluated at the site j. With an appropriate choice of the short-range interaction parameters and a change of variables from real space $\boldsymbol{\xi}_j$ and ϕ_j to Fourier space $\boldsymbol{\xi}(\boldsymbol{q})$ and $\phi(\boldsymbol{q})$, it is straightforward to show that integration over the auxiliary fields $\phi(\boldsymbol{q})$ generates a quadratic interaction in the $\boldsymbol{\xi}$ that reproduces not only the leading-order non-analytic behaviour of the dipolar interaction $A^{\alpha\beta}(\boldsymbol{q})$ as $q\to 0$ (Aharony & Fisher 1973),

$$A^{\alpha\beta}(\boldsymbol{q})=a_1\frac{q^\alpha q^\beta}{q^2}-a_2q^\alpha q^\beta-[a_3+a_4q^2-a_5(q^\alpha)^2]\delta_{\alpha\beta}+\mathcal{O}((q^\alpha)^4,(q^\alpha)^2(q^\beta)^2,q^4,\ldots),$$

PHILOSOPHICAL TRANSACTIONS OF THE ROYAL SOCIETY A MATHEMATICAL, PHYSICAL & ENGINEERING SCIENCES

but, to an excellent approximation, the whole function $A^{\alpha\beta}(\boldsymbol{q})$ throughout the Brillouin zone as computed using the Ewald method. There is, however, a catch. This is that the interaction term $i\mathcal{H}_{\text{int}}$ must be purely imaginary due to the sign of the Fourier transform of the dipole interaction matrix, and thus the 'partition function' and related integrals for the extended system cannot be evaluated with a simple Metropolis Monte Carlo method. If there were an efficient numerical approach for evaluating these integrals, this method could be competitive with existing fast-multipole algorithms, especially in systems with periodic boundary conditions. Work to identify a suitable algorithm is in progress.

5. Finite temperature simulations: method and results

For the investigation of the ferroelectric transition in $PbTiO_3$, we use a single-flip Metropolis approach, with runs ranging between 25 000 and 150 000 sweeps through the lattice. Periodic boundary conditions are imposed on an $L \times L \times L$ simulation cell, with finite-size scaling applied for L ranging from 5 to 11. In a finite-size simulation, a first-order transition such as the ferroelectric transition in $PbTiO_3$ leads to the coexistence of two distinct phases, separated by an energy barrier, in a temperature range near T_c. Recently developed Monte Carlo methods for first-order transitions (Berg & Neuhaus 1992; Borgs & Janke 1992; Janke 1992) determine the transition temperature from the condition that the difference in the free energies of the two phases be zero. If the two phases are sampled ergodically in the simulation, this difference is quite easy to compute. However, in general first-order transitions, unbiased sampling of the two phases can be extremely difficult to achieve, especially as the simulation-cell size increases. While we are presently considering various algorithms suitable for this situation, for now we put bounds on T_c by monitoring the sensitivity of the average structural parameters to the choice of initial state: $T_>$ is the lowest temperature at which the system averages are characteristic of the cubic state, starting with an initial ground state tetragonal configuration, while $T_<$ is the highest temperature at which a starting cubic configuration results in a tetragonal state. These bounds are plotted in figure 1. A value of $T_c = 660$ K, obtained from averaging the bounds at the largest system size, is in very good agreement with the experimental transition temperature 763 K.

From the Monte Carlo simulations, we obtained additional information about the behaviour at the transition. An estimate of a latent heat of 3400 J mol^{-1}, extracted from separate runs for the two phases at $L = 9$, obtained by using different initial states at $T = 666$ K, is in rough agreement with the measured value of 4800 J mol^{-1} (Shirane & Sawaguchi 1951), and very much larger than the 209 J mol^{-1} latent heat of the cubic–tetragonal transition in $BaTiO_3$ (Shirane & Takeda 1952). The discontinuous change in the structural parameters through the first-order transition can be seen in figures 2 and 3, slightly broadened by the finite-size effects.

One of the unique opportunities offered by this first-principles analysis is to investigate the role of different contributions to $\mathcal{H}_{\text{eff}}$ by performing simulations in which individual terms have been 'turned off'. One particularly striking result of this procedure is that if the homogeneous strain coupling parameters g_0, g_1 and g_2 are set to zero, the character of the transition changes significantly. The transition temperature, determined using cumulants at several system sizes, shifts significantly downward to a value of 400 K. The temperature dependence of the average uniform local distortion shows no jump, but rather a smooth increase through the transition,

PHILOSOPHICAL TRANSACTIONS OF THE ROYAL SOCIETY A MATHEMATICAL, PHYSICAL & ENGINEERING SCIENCES

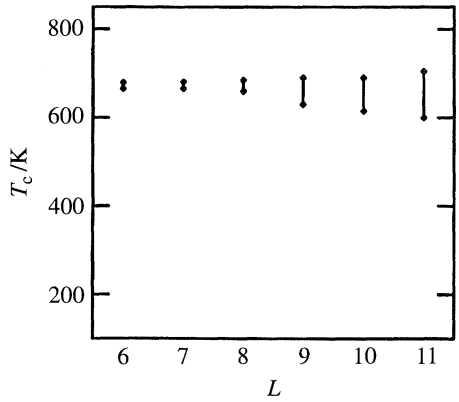

Figure 1. Monte Carlo estimate of T_c as a function of increasing simulation-cell size L. At each L, the vertical line extends from the lower bound $T_<$ to the upper bound $T_<$, calculated as described in the text.

Figure 2

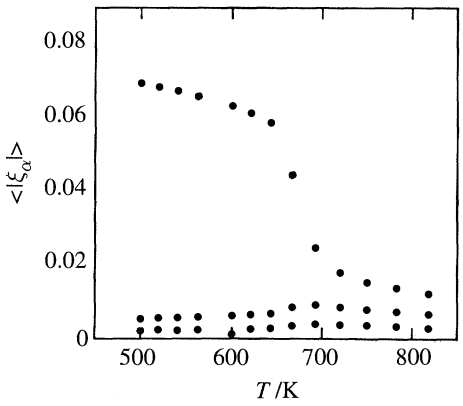

Figure 3

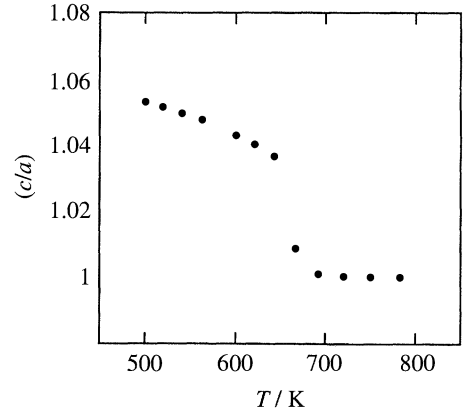

Figure 2. The thermally averaged absolute values of the largest, middle and smallest components of $(1/N)\sum_i \boldsymbol{\xi}_i$ are plotted as a function of temperature in the vicinity of the calculated transition temperature $T_c = 660$ K. The simulation was performed for $L = 5$, with 90 000 Monte Carlo sweeps at each temperature.

Figure 3. The thermal average of the tetragonal unit cell distortion c/a is plotted as a function of temperature in the vicinity of the calculated transition temperature $T_c = 660$ K, from the same simulation as in figure 2.

as expected for a finite-size simulation of a second-order transition. Furthermore, the low-temperature phase is not tetragonal, but rhombohedral. From this observed change in character from a first-order cubic–tetragonal transition to a second-order cubic–rhombohedral transition, we conclude that not only is the strain coupling responsible for stabilizing the ground-state tetragonal structure, as has been previously noted (Cohen & Krakauer 1992; Cohen 1992), but it is also the key factor in producing the pronounced first-order character of the ferroelectric transition in $PbTiO_3$.

To investigate in more detail how strain coupling affects the order of the transition and stabilizes particular phases, we have applied the mean field theory technique, where the role played by individual parameters can be analytically examined. The comparison with Monte Carlo results also permits us to assess the role of fluctuations in determining transition behaviour. Here, we present a mean field theory analysis

of the effective Hamiltonian valid for ferroelectrics both of the types $PbTiO_3$ and types $BaTiO_3$ and $KNbO_3$, including strain coupling. In the variational formulation, a trial density matrix is used to evaluate the free energy functional

$$F[\hat{\rho}] = \mathrm{tr}[\hat{\rho}\mathcal{H}] + kT\,\mathrm{tr}[\hat{\rho}\ln\hat{\rho}],$$

which is then minimized with respect to the variational parameters. In the present case, the trial density matrix corresponding to mean field theory has the form of the product of independent single-site density matrices

$$\hat{\rho}[\{\boldsymbol{\xi}_i\},\boldsymbol{v},\boldsymbol{e};\boldsymbol{h},\boldsymbol{\chi},\boldsymbol{\phi}] = \frac{\exp(-\beta[\mathcal{H}_{\mathrm{str},1}(\boldsymbol{v},\boldsymbol{e};\boldsymbol{\chi},\boldsymbol{\phi})])}{Z_{s,1}}\prod_i \frac{\exp(-\beta[\mathcal{H}_1(\boldsymbol{\xi}_i;\boldsymbol{h},Q_{\alpha\beta}])}{Z_1},$$

where

$$\mathcal{H}_{\mathrm{str},1}(\boldsymbol{v},\boldsymbol{e};\boldsymbol{\chi},\boldsymbol{\phi}) = \tfrac{1}{2}(C_{11}+2C_{12})v_1^2 + \tfrac{1}{2}(C_{11}-C_{12})(v_2^2+v_3^2) + 2C_{44}(e_1^2+e_2^2+e_3^2) + \boldsymbol{\chi}\cdot\boldsymbol{v} + \boldsymbol{\phi}\cdot\boldsymbol{e},$$

$$Z_{s,1} = \int \mathrm{d}\boldsymbol{v}\,\mathrm{d}\boldsymbol{e}\exp(-\beta\mathcal{H}_{\mathrm{str},1}), \quad Z_1 = \int \mathrm{d}\boldsymbol{\xi}\exp(-\beta\mathcal{H}_1),$$

$$\mathcal{H}_1(\boldsymbol{\xi};\boldsymbol{h},Q_{\alpha\beta}) = V_{\mathrm{loc}}(\boldsymbol{\xi}) + \boldsymbol{\xi}\cdot\boldsymbol{h} - \sum_{\alpha\leqslant\beta} Q_{\alpha\beta}\xi_\alpha\xi_\beta.$$

A simplified notation has been introduced for the strain degrees of freedom, that is $v_1 = (1/\sqrt{3})(e_{xx}+e_{yy}+e_{zz})$, $v_2 = (1/\sqrt{2})(e_{xx}-e_{yy})$, $v_3 = (1/\sqrt{6})(-e_{xx}-e_{yy}+2e_{zz})$, $e_1 = e_{xy}$, $e_2 = e_{xz}$, and $e_3 = e_{yz}$. Each $\mathcal{H}_1$ factor in the trial density matrix is the probability distribution for a single vector $\boldsymbol{\xi}$ in an effective field generated by the nonzero average values of the neighbouring vectors and an effective potential due to the homogeneous strain. For the strain, the additional $\mathcal{H}_{\mathrm{str},1}$ factor in the trial density matrix is the probability distribution of the components of the homogeneous strain under an effective stress generated by the nonzero average values of the squared vectors. The effective field $\boldsymbol{h}$ and the effective stresses $\boldsymbol{\chi}$ and $\boldsymbol{\phi}$ are the variational parameters. The effective potential tensor $Q_{\alpha\beta}$ is not an independent variational quantity, but is determined by the strain coupling terms in $\mathcal{H}$ and the homogeneous strain produced by the effective stresses $\boldsymbol{\chi}$ and $\boldsymbol{\phi}$, so that

$$Q_{xx} = -\left(\frac{\sqrt{3}\tilde{b}\chi_1}{C_{11}+2C_{12}} + \frac{\tilde{a}}{\sqrt{2}(C_{11}-C_{12})}\left(\chi_2 - \frac{1}{\sqrt{3}}\chi_3\right)\right),$$

$$Q_{yy} = -\left(\frac{\sqrt{3}\tilde{b}\chi_1}{C_{11}+2C_{12}} - \frac{\tilde{a}}{\sqrt{2}(C_{11}-C_{12})}\left(\chi_2 + \frac{1}{\sqrt{3}}\chi_3\right)\right),$$

$$Q_{zz} = -\left(\frac{\sqrt{3}\tilde{b}\chi_1}{C_{11}+2C_{12}} + \frac{2\tilde{a}}{\sqrt{6}(C_{11}-C_{12})}\chi_3\right),$$

$$Q_{xy} = -\frac{g_2}{4C_{44}}\phi_1, \quad Q_{xz} = -\frac{g_2}{4C_{44}}\phi_2, \quad Q_{yz} = -\frac{g_2}{4C_{44}}\phi_3,$$

where $\tilde{a} = g_1$ and $\tilde{b} = g_0 + \frac{1}{3}g_1$.

After considerable rearrangement, the free energy functional takes the form

$$-kT\ln Z_1 + \langle\boldsymbol{\xi}\rangle\cdot\boldsymbol{h} + \frac{A_s}{2N}\sum_\alpha\langle\xi_\alpha\rangle^2 + \frac{\chi_1^2}{2(C_{11}+2C_{12})} + \frac{(\chi_2^2+\chi_3^2)}{2(C_{11}-C_{12})} + \frac{(\phi_1^2+\phi_2^2+\phi_3^2)}{8C_{44}}.$$

The resulting extremum equations can be examined to show the equivalence of this analysis to the usual self-consistent equations of mean field theory; in particular, $\boldsymbol{h} = A_s\langle\boldsymbol{\xi}\rangle$. In our approach, the trial free energy functional is minimized numerically using conjugate-gradients minimization and three-dimensional integration subroutines from IMSL. We compute the free energies as a function of temperature separately for the cubic phase (one variational parameter), the tetragonal phase (three variational parameters) and the rhombohedral phase (three variational parameters). We find that for the full $PbTiO_3$ Hamiltonian the cubic phase is most stable above $T_c = 1100$ K, while for temperatures below T_c the tetragonal phase is more stable than the rhombohedral phase, and both are lower in free energy than the cubic phase (which is not necessarily locally stable). For the $PbTiO_3$ Hamiltonian with strain coupling set to zero, the transition temperature shifts considerably downward, to $T_c = 910$ K, and the rhombohedral phase is now seen to be the most stable phase for temperatures below T_c. While, as is not unexpected, the mean-field transition temperatures are significantly higher than those obtained in the Monte Carlo simulations, the magnitude of the shift is similar and the same low-temperature phases are observed in both approaches.

To determine the order of the transition in our mean field analysis, we focus on the point where the cubic and low symmetry phase free energy curves cross. The behaviour in the vicinity of this temperature can be described by a Landau free energy functional. In this framework, the minimization of the strain variational parameters induces an anisotropic negative fourth-order interaction favouring the tetragonal phase. If this is large enough to lead to an overall negative fourth-order term it will, within Landau theory, produce the triple-well potential associated with a first-order transition. Surprisingly, we find within our computational accuracy that both the zero strain and full Hamiltonian transitions are second order in mean field theory. This may be related to the observation that the structural parameters for the tetragonal phase in figures 2 and 3 smoothly extrapolate to zero at around the mean field transition temperature. Thus, we speculate that the transition is driven first order by strain-coupled fluctuations, in a manner similar to that previously discussed for the structural transition in GeTe (Rabe & Joannopoulos 1987*a*, *b*, 1992), and more recently in Salje & Vallade (1994).

It may be much more generally true for the perovskites that strain plays an essential role in producing a first-order cubic–tetragonal transition in systems which would otherwise have rhombohedral ground states. For example, the effect of setting strain coupling to zero in $BaTiO_3$ is similar to what we have described previously, with the correct phase sequence and transition orders being replaced by a direct cubic–rhombohedral transition (Zhong *et al.* 1994*b*, 1995). To test this idea further, we have used mean-field theory to analyse the eight-site model of Comes (1968), introduced for the interpretation of diffraction results in $BaTiO_3$ and generally regarded as providing a plausible scenario for the observed sequence of phase transitions. This model can be regarded as a limiting case of our vector model, where V_{loc} possesses such deep wells along the (111) directions that the only allowed values for the vector on each site are $\xi_0(\pm1, \pm1, \pm1)$, while the intersite interactions retain the same form as in expressions (2.1)–(2.4). In this model, the entropy is purely configurational, with the largest entropy in the cubic phase (equal probability for the site in each of the eight sites), followed by the tetragonal phase (four sites preferentially occupied with equal probability), the orthorhombic phase (two preferred sites) and the rhombohedral phase (one preferred site). The energy follows the opposite order, with the

PHILOSOPHICAL TRANSACTIONS OF THE ROYAL SOCIETY A MATHEMATICAL, PHYSICAL & ENGINEERING SCIENCES

rhombohedral phase (allowing maximal lineup of spins on neighbouring sites) most favourable in energy, and the cubic phase least. It is these opposite trends in energy and entropy that are generally assumed to lead to the observed sequence of phases (cubic–tetragonal–orthorhombic–rhombohedral) with decreasing temperature.

In fact, a quantitative calculation of the phase diagram, in mean field theory, shows this model undergoing a direct cubic–rhombohedral transition, with no intermediate tetragonal or orthorhombic phases. The calculation is a simple special case of the mean field theory we have described previously, since the V_{loc} term in the local potential contributes no structural dependence. It follows that the trial free energy decouples into a sum of the trial free energies for three independent Ising models, each separately determining one Cartesian component of the effective field $\boldsymbol{h}$. Since the tetragonal phase corresponds to one non-zero component of $\boldsymbol{h}$, and the rhombohedral phase corresponds to the three components being equal in magnitude and non-zero, it is clear that the latter phase must always be more stable than the former. This conclusion is preserved by the use of the most general single-site trial density matrix for the eight-site model, which for the tetragonal phase does not introduce any additional variational parameters and therefore does not result in any lowering of its free energy. While awaiting a full treatment of the eight-site model (for example, results of Monte Carlo simulations), we speculate that the character of the transition can only be changed by extending the model to include strain coupling. Investigations of this issue are in progress.

The mechanism for the observed sequence of transitions in the ferroelectric perovskites has long been a central issue in the study of these materials. Here, we have identified important roles both for strain coupling and fluctuations in producing the correct low temperature phases and orders for the transition. Further support comes from the recent work of Cowley, who found that general vector models on a simple cubic lattice with quadratic intersite interactions do not, within mean field theory, exhibit the sequence of first-order cubic–tetragonal–orthorhombic–rhombohedral transitions characteristic of $BaTiO_3$ (Cowley 1995). Indeed, as we have shown previously, even the canonical eight-site model does not provide a mechanism for the transition sequence within mean field theory without strain coupling. The explicit inclusion of strain provides a mechanism for stabilizing a tetragonal phase in a system which would otherwise have a rhombohedral ground state. However, with values for model parameters obtained for $PbTiO_3$ from first principles, the first-order character of the cubic–tetragonal transition is not reproduced in the mean field theory. The fact that the correct behaviour is only observed for the $PbTiO_3$ model in numerical Monte Carlo simulations only when strain coupling is included suggest that the effects of strain-coupled fluctuations are essential in producing the observed first-order character of the transition, as discussed in Salje & Vallade (1994). Furthermore, at present we have not been able to find a set of model parameters which yields a cubic–tetragonal–orthorhombic–rhombohedral sequence in mean field theory. Thus intersite fluctuations combined with strain coupling may be responsible for stabilizing a tetragonal phase at intermediate temperatures. We speculate that the same conclusion holds for other ferroelectrics such as $KNbO_3$ and $BaTiO_3$. It is even possible that these two effects stabilize a transition into the tetragonal phase from the cubic phase for a broad class of parameter values, providing an explanation of the experimental non-observation of direct cubic-rhombohedral transitions in stoichiometric perovskite compounds (Cohen 1995).

PHILOSOPHICAL TRANSACTIONS OF THE ROYAL SOCIETY A MATHEMATICAL, PHYSICAL & ENGINEERING SCIENCES

6. Future directions

Spatial fluctuations and transformation-induced microstructure effects in ferroelastics have been the subject of recent research on the microscopic level (Marais *et al.* 1994; Parlinski *et al.* 1993*a*, *b*). In ferroelectrics, spatial inhomogeneity and domain structure are also considered to play an important role in the experimentally observed behaviour (Zhang *et al.* 1994). Many of the issues that arise have direct analogs in ferroelastics. However, in ferroelectric systems, we have the additional factor of long-range dipolar interactions which we expect will compete (or cooperate) with the strain-induced interactions to produce characteristic microstructure effects. Therefore, microscopic investigations based on realistic effective Hamiltonians for microstructural effects in ferroelectrics are of great interest. In such simulations, the quantitative balance of the competing interactions could be meaningfully examined, and the separate roles of the various energetic contributions identified by selectively turning them off.

Direct simulations with the full microscopic Hamiltonian on a sufficiently large scale for these investigations are extremely computationally demanding. The largest sizes ($12 \times 12 \times 12$ unit cells) used in our Monte Carlo simulations of the phase transition are certainly too small to contain more than one domain. In particular, we found that setting the coupling to inhomogeneous strain to zero has negligible effects on the properties of the structural transition. As discussed in § 4, the improvement of algorithms for evaluating dipolar energies should relax these size limitations. In addition, it is necessary to examine the effects of different boundary conditions, most notably free boundary conditions and periodic boundary conditions. Lastly, dynamical effects should be also be included in the investigation. Because of the simple form of the kinetic energy in effective Hamiltonians constructed by the lattice Wannier function method, this can be readily accomplished by using an appropriate molecular dynamics method. Work towards dynamical simulations is in progress.

Since the largest simulation size attainable for the full microscopic Hamiltonian will be limited even with significant improvements in the algorithms, it is worthwhile to consider alternative approaches to the quantitative studies of microstructure in individual ferroelectric materials. The most natural approach is to use the full microscopic Hamiltonian as the starting point for the derivation of a realistic coarse-grained model, which is then applied to the phenomena of interest. For example, time-dependent Ginzburg–Landau theory, with empirically derived parameters, has been widely applied to the study of domain wall profiles and motion (Houchmandzadeh *et al.* 1991), and more generally to transformation-related microstructures (Tsatskis *et al.* 1994). Just as we can obtain the parameters in a Landau theory of the ferroelectric transition from first principles, we could generalize this procedure to derive Ginzburg–Landau gradient terms and relaxation times from our first-principles effective Hamiltonian. This would not only permit the extension of simulation studies to much larger system sizes, but also allow the quantitative evaluations of approximations made in the Ginzburg–Landau form through computation of the neglected terms and direct comparison with small-scale simulations. Through this connection to the extensive literature on continuum approaches to transformation-induced strain effects, substantial progress in the understanding of individual ferroelectric materials can be expected.

PHILOSOPHICAL TRANSACTIONS OF THE ROYAL SOCIETY A MATHEMATICAL, PHYSICAL & ENGINEERING SCIENCES

7. Conclusions

First-principles calculations of total energy and force constants, combined with the construction of an effective Hamiltonian, provide a quantitative approach to the investigation of strain-related effects at the finite-temperature ferroelectric transition in $PbTiO_3$. Such effects appear to play an essential role in producing the correct character for the transition and low-temperature phase in $PbTiO_3$, and there is reason to believe that this is true for other perovskite compounds as well. Future extensions to larger-scale simulations and investigation of dynamical properties can be expected to yield further information about the role of strain coupling in determining the properties of ferroelectric perovskites and related materials.

We are grateful to R. E. Cohen, E. R. Cowley, V. Heine, and E. K. H. Salje for useful discussions and valuable assistance. We thank M. C. Payne and V. Milman for the use of CASTEP 2.1. This work was supported by ONR Grant N00014-91-J-1247. In addition, K.M.R. acknowledges the support of the Clare Boothe Luce Fund and the Alfred P. Sloan Foundation.

References

Aharony, A. & Fisher, M. E. 1973 *Phys. Rev.* B **8**, 3323, appendix A.

Allen, M. P. & Tildesley, D. J. 1987 *Computer simulation of liquids*, ch. 4. Oxford.

Berg, B. A. & Neuhaus, T. 1992 Multicanonical ensemble: a new approach to simulate first-order phase transitions. *Phys. Rev. Lett.* **68**, 9–12.

Borgs, C. & Janke, W. 1992 New method to determine first-order transition points from finite-size data. *Phys. Rev. Lett.* **68**, 1738–1741.

Bratkovsky, A. M., Salje, E. K. H., Marais, S. C. & Heine, V. 1994 Theory and computer simulation of tweed texture. *Phase Transitions* **48**, 1–13.

Cochran, W. & Zia, A. 1968 Structure and dynamics of perovskite-type crystals. *Phys. Stat. Sol.* **25**, 273–283.

Cohen, R. E. 1992 Origin of ferroelectricity in perovskite oxides. *Nature* **358**, 136–138.

Cohen, R. E. & Krakauer, H. 1992 Electronic structure studies of the differences in ferroelectric behaviour of $BaTiO_3$ and $PbTiO_3$. *Ferroelectrics* **136**, 65–83.

Comes, R., Lambert, M. & Guinier, A. 1968 The chain structure of $BaTiO_3$ and $KNbO_3$. *Solid State Commun.* **6**, 715–719.

Cowley, E. R. 1995 Molecular field models for ferroelectric crystals. *Ferroelectrics* **164**, 123–131.

Ghosez, Ph., Gonze, X. & Michenaud, J.-P. 1994 First principles calculations of dielectric and effective charge tensors in barium titanate. *Ferroelectrics* **153**, 91–96.

Janke, W. 1992 Accurate first-order transition points from finite-size data without power-law corrections. *Phys. Rev.* B **47**, 14 757–14 770.

Keating, P. N. 1966 Effect of invariance requirements on the elastic strain energy of crystals with application to the diamond structure. *Phys. Rev.* **145**, 637–645.

King-Smith, R. D. & Vanderbilt, D. 1994 First-principles investigation of ferroelectricity in perovskite compounds. *Phys. Rev.* B **49**, 5828–5844.

Krakauer, H. & Yu, R. 1995 First-principles determination of chain-structure instability in $KNbO_3$. *Phys. Rev. Lett.* **74**, 4067–4070.

Lines, M. E. & Glass, A. M. 1977 *Principles and applications of ferroelectrics and related materials*, ch. 8. Oxford: Clarendon Press.

Marais, S., Heine, V., Nex, C. & Salje, E. 1991 Phenomena due to strain coupling in phase transitions. *Phys. Rev. Lett.* **66**, 2480–2483.

Marais, S., Salje, E., Heine, V. & Bratkovsky, A. 1994 Strain-related microstructures in materials: a computer simulation study of a simple model. *Phase Transitions* **48**, 15–45.

Parlinski, K., Heine, V. & Salje, E. K. H. 1993*a* Origin of tweed texture in the simulation of a cuprate superconductor. *J. Phys.* C **5**, 497–518.

Parlinski, K., Salje, E. K. H. & Heine, V. 1993*b* Annealing of tweed microstructure in high T_c superconductors studied by a computer simulation. *Acta Metall. Mater.* **41**, 839–847.

Posternak, M., Resta, R. & Baldereschi, A. 1994 Role of covalent bonding in the polarization of perovskite oxides: the case of $KNbO_3$. *Phys. Rev.* B **50**, 8911–8914.

Postnikov, A. V. & Borstel, G. 1994 Γ phonons and microscopic structure of orthorhombic $KNbO_3$ from first-principles calculations. *Phys. Rev.* B **50**, 16 403–16 409.

Postnikov, A. V., Neumann, T. & Borstel, G. 1994 Phonon properties of $KNbO_3$ and $KTaO_3$ from first-principles calculations. *Phys. Rev.* B **50**, 758–763.

Rabe, K. M. & Joannopoulos, J. D. 1987*a* *Ab initio* determination of a structural phase transition temperature. *Phys. Rev. Lett.* **59**, 570.

Rabe, K. M. & Joannopoulos, J. D. 1987*b* Theory of the structural transition of GeTe. *Phys. Rev.* B **36**, 6631.

Rabe, K. M. & Joannopoulos, J. D. 1992 *Ab initio* statistical mechanics of structural phase transitions. In *Electronic phase transitions* (ed. W. Hanke & Y. V. Kopaev), ch. 3. Amsterdam: North-Holland.

Rabe, K. M. & Waghmare, U. V. 1994 First-principles model Hamiltonians for ferroelectric phase transition. *Ferroelectrics* **151**, 59–68.

Rabe, K. M. & Waghmare, U. V. 1995*a* Ferroelectric phase transitions: a first principles approach. *Ferroelectrics* **164**, 15–32.

Rabe, K. M. & Waghmare, U. V. 1995*b* Localized basis for effective lattice Hamiltonians: lattice Wannier functions. *Phys. Rev.* B **52**, 13 236-13 246.

Rabe, K. M. & Waghmare, U. V. 1996 Ferroelectric phase transitions from first principles. *J. Phys. Chem. Solids.* (In the press.)

Salje, E. K. H. 1990 *Phase transitions in ferroelastic and coelastic crystals.* Cambridge University Press.

Salje, E. K. H. 1992 Application of Landau theory for the analysis of phase transitions in minerals. *Phys. Rep.* **215**, 49–99.

Salje, E. K. H. & Vallade, M. 1994 *J. Phys.* C **6**, 5601.

Shirane, G. & Sawaguchi, E. 1951 On the anomalous specific heat of lead titanate. *Phys. Rev.* **81**, 458-459.

Shirane, G. & Takeda, A. 1952 *J. Phys. Soc. Jap.* **7**, 1.

Singh, D. J. 1995 Structure and energetics of antiferroelectric $PbZrO_3$. *Phys. Rev.* B **52**, 12 559-12 563.

Singh, D. J. & Boyer, L. L. 1992 First principles analysis of vibrational modes in $KNbO_3$. *Ferroelectrics* **136**, 95–103.

Tsatskis, I., Vul, D. A., Salje, E. K. H. & Heine, V. 1994 Geometrical coupling between inhomogeneous strain fields: application to fluctuations in ferroelectrics. *Phase Transitions* **52**, 95–107.

Waghmare, U. V. & Rabe, K. M. 1996 Lattice instabilities, anharmonicity and phase transitions in $PbZrO_3$ from first principles. *Ferroelectrics.* (In the press.)

Zhang, Q. M., Wang, H., Kim, N. & Cross, L. E. 1994 Direct evaluation of domain-wall and intrinsic contributions to the dielectric and piezoelectric response and their temperature dependence on lead zirconate-titanate ceramics. *J. App. Phys.* **75**, 454–459.

Zhong, W. & Vanderbilt, D. 1995 Competing structural instabilities in cubic perovskites. *Phys. Rev. Lett.* **74**, 2587–2590.

Zhong, W, King-Smith, R. D. & Vanderbilt, D. 1994*a* Giant LO–TO splittings in perovskite ferroelectrics. *Phys. Rev. Lett.* **72**, 3618–3621.

Zhong, W., Vanderbilt, D. & Rabe, K. M. 1994*b* Phase transitions in $BaTiO_3$ from first principles. *Phys. Rev. Lett.* **73**, 1861–1864.

Zhong, W., Vanderbilt, D. & Rabe, K. M. 1995 First-principles theory of ferroelectric phase transitions for perovskites: the case of $BaTiO_3$. *Phys. Rev.* B **52**, 6301–6312.

PHILOSOPHICAL TRANSACTIONS OF THE ROYAL SOCIETY A MATHEMATICAL, PHYSICAL & ENGINEERING SCIENCES